

MAMOC: MRI Motion Correction via Masked Autoencoding

Lennart Alexander Van der Goten^{1,2}

lavdg@kth.se

Jingyu Guo^{1,2}

jingyug@kth.se

Kevin Smith^{1,2}

ksmith@kth.se

for the Alzheimer’s Disease Neuroimaging Initiative[‡]

¹KTH Royal Institute of Technology, Stockholm, SWEDEN

²Science for Life Laboratory, Solna, SWEDEN

Abstract

The presence of motion artifacts in magnetic resonance imaging (MRI) scans poses a significant challenge, where even minor patient movements can lead to artifacts that may compromise the scan’s utility. This paper introduces **MA**ske**D** **MO**tion **C**orrection (MAMOC), a novel method designed to address the issue of Retrospective Artifact Correction (RAC) in motion-affected MRI brain scans. MAMOC uses masked autoencoding self-supervision, transfer learning and test-time prediction to efficiently remove motion artifacts, producing high-fidelity, native-resolution scans. Until recently, realistic, openly available paired artifact presentations for training and evaluating retrospective motion correction methods did not exist, making it necessary to simulate motion artifacts. Leveraging the MR-ART dataset and bigger unlabeled datasets (ADNI, OASIS-3, IXI), this work is the first to evaluate motion correction in MRI scans using real motion data on a public dataset, showing that MAMOC achieves improved performance over existing motion correction methods.

1 Introduction

Artifacts pose a serious challenge when it comes to magnetic resonance imaging (MRI). Performing an MRI scan is usually a costly endeavor as it requires specially-trained personnel, expensive highly-advanced medical equipment, and long scan durations. Commonly occurring artifacts (e.g., motion, ghosting, bias fields, etc.) can cause a scan to become impossible to read, forcing healthcare providers to perform the procedure anew. Being able to filter out or correct artifacts (see Fig. 1) is therefore of particular interest as it not only saves costs but also reduces discomfort in patients, especially when the artifact cannot be prevented (e.g., due to Parkinson’s disease, stroke, cardiac motion).

In this work, we propose MAMOC (**MA**ske**D** **MO**tion **C**orrection), which tackles the Retrospective Artifact Correction (RAC) task specifically on *motion-affected* MRI scans. It leverages

[‡] Data used in preparation of this article were obtained from the Alzheimer’s Disease Neuroimaging Initiative (ADNI) database (adni.loni.usc.edu). As such, the investigators within the ADNI contributed to the design and implementation of ADNI and/or provided data but did not participate in analysis or writing of this report. A complete listing of ADNI investigators can be found at: http://adni.loni.usc.edu/wp-content/uploads/how_to_apply/ADNI_Acknowledgement_List.pdf

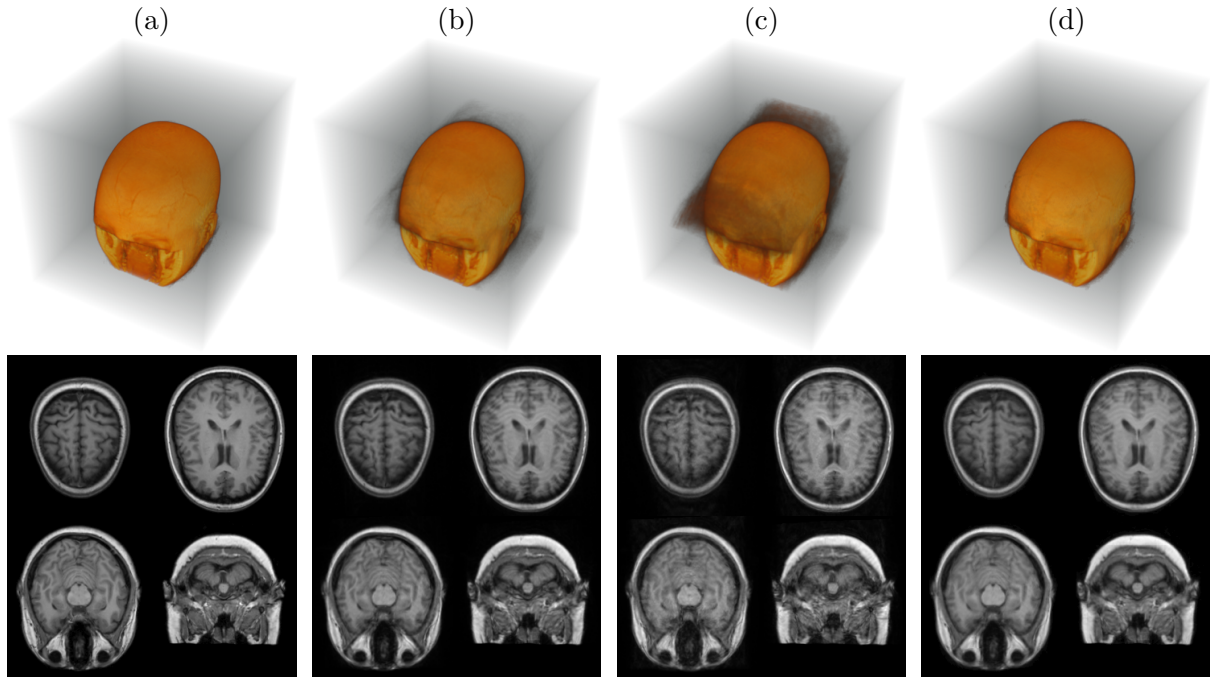


Figure 1: **Varying Levels of Head Motion.** 3D & 2D renderings of the same subject from the MR-ART dataset with (a) no head motion, (b) moderate head motion and (c) heavy head motion, (d) motion-corrected with MAMOC

the novel MR-ART [Nárai et al., 2022] corpus, the first-of-its-kind dataset to provide multiple MRI brain scans per patient taken during the same session, with moderate motion, heavy motion, and a clean scan. The small size of MR-ART, 148 patients, makes it challenging to directly train a supervised model to correct motion artifacts, but it still provides unique value as a tool to evaluate RAC methods on realistic motion data instead of simulations. To overcome the size limitation, we use self-supervision driven by *masked autoencoding* [He et al., 2022] to learn the manifold of motion-unaffected data from several large, highly-curated datasets: ADNI [Wyman et al., 2013], OASIS-3 [LaMontagne et al., 2019] and IXI [Brain Development.org, 2023]. We then apply transfer learning on the limited labeled information available from the available from MR-ART.

Our contributions can be listed as follows:

1. We propose a novel approach to remove motion artifacts from MR imagery using masked autoencoding self-supervision and transfer learning, MAMOC.
2. We show that masked autoencoding in MAMOC can be used at inference time to improve the quality of reconstruction.
3. MAMOC is able to synthesize native resolution motion-corrected MR imagery corresponding to voxel sizes of 1mm^3 , 256^3 voxels.
4. We compare MAMOC to existing methods on *real motion artifacts* from MR-ART, and demonstrate state-of-the-art performance w.r.t. image quality metrics, structural similarity, and a downstream subcortical segmentation task.

2 Related Work

2D Image Restoration & Generative Modeling

Image restoration is a type of inverse problem concerned with the automatic removal of artifacts from imagery [Lehtinen et al., 2018, Zhang et al., 2017]. Many modern works in this domain follow a holistic approach and are able to remove a wide class of artifacts [Lehtinen et al., 2018, Liang et al., 2021] from imagery. While early research relied on handcrafted features, more recent approaches often adopt fully-learnable generative models [Küstner et al., 2019, Wu et al., 2021]. In some recent works [Liang et al., 2021, Xiao et al., 2023] established convolutional elements have been supplanted with transformer-based architectures, allowing them to model larger contexts which can be advantageous for removing certain types of artifacts.

Prospective Artifact Correction

Prospective Artifact Correction (PAC) refers to approaches that are concerned with either preventing artifacts altogether or by gathering sufficient information to remove artifacts in real-time [Maclaren et al., 2013]. Motion artifacts can be minimized by encouraging patients to remain still during the scan through clear instructions and by providing a comfortable scanning environment. In some cases, light sedation or other medical interventions [Spieker et al., 2023] may be necessary, but these should be used judiciously and with the patient’s well-being in mind. Sensoric methods [Herbst et al., 2011, Zaitsev et al., 2006] utilize additional data sources to dynamically correct motion artifacts, offering a non-invasive alternative to physical restraints. They typically assume motion rigidity and may extend scan durations, potentially increasing patient discomfort [Maclaren et al., 2013].

Retrospective Artifact Correction

Retrospective Artifact Correction (RAC) methods seek to remove artifacts *after* acquisition without relying on additional data [Spieker et al., 2023]. RAC methods can typically be divided into two subfields: (i) k -space based and (ii) image-based. The former category operates directly in the k -space – the frequency space which is the precursor to MR image space. The latter category takes motion-affected scans (post-reconstruction) as input and aims to produce a scan that features fewer pronounced artifacts. Given the limited availability of k -space data [Noordman et al., 2023], our approach focuses on the image-based domain. Image-based works can be further categorized based on the generative modeling approach they utilize, such as Variational Autoencoders (VAEs) [Küstner et al., 2019] and GANs [Wu et al., 2021]. In addition to generative models, supervised methods [Lyu et al., 2021, Van der Goten and Smith, 2022] utilize motion artifact simulators to generate paired scans to restore the image. These methods leverage the availability of simulated data to train models for specific tasks, thereby providing a practical solution to the challenges posed by the absence of paired real-world data. MAMOC relies on a very limited amount of supervised training data containing *real* motion artifacts, not simulations. Because the amount of supervised data is too small to train a model from scratch, MAMOC uses a self-supervised pre-training strategy that leverages large-scale, highly-curated datasets, to learn features for generating high-quality MRI imagery.

3 Method

In the following section, we describe how we design MAMOC to effectively filter out motion artifacts, taking advantage of self-supervision and transfer learning on large, artifact-free datasets to be able to learn to correct real motion artifacts from limited supervised data in MR-ART.

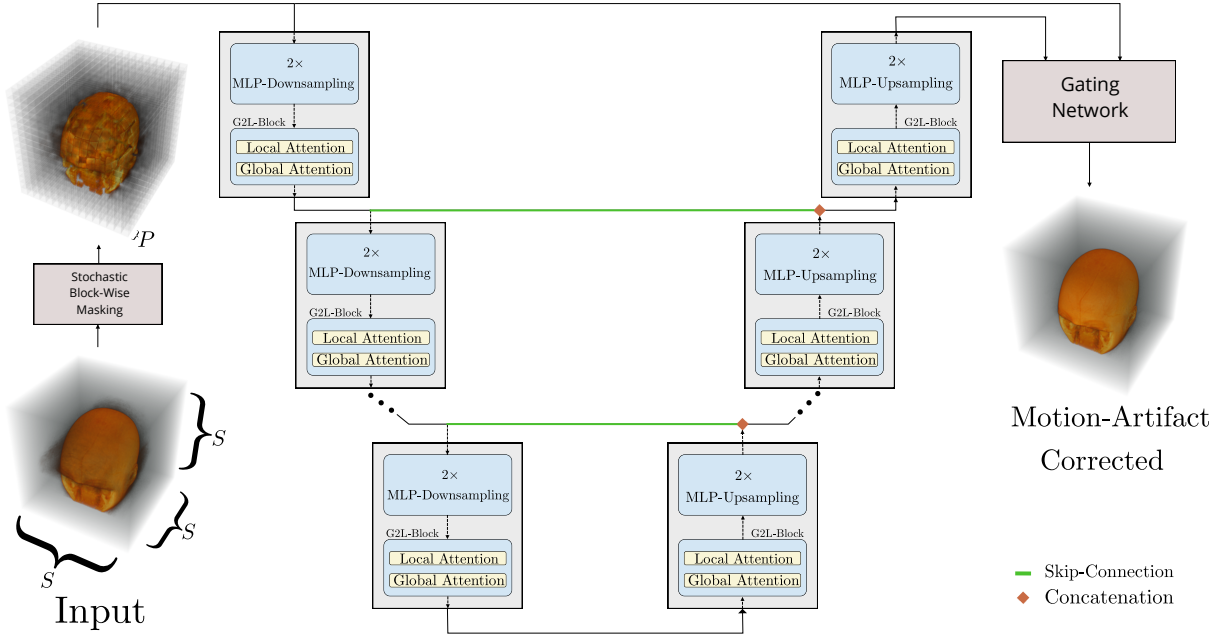


Figure 2: **Architecture.** MAMOC arranges G2L transformer blocks in a U-Net-like structure, featuring a contracting encoder path and an expanding decoder path connected by skip connections and a bottleneck layer. During training and inference, inputs are randomly masked for reconstruction. A gating network learns which voxels from the masked input can be preserved and passed to the output.

Architecture

We adopt a U-Net-like architecture [Ronneberger et al., 2015], featuring a contracting encoder path successively producing coarser resolutions, and an expanding decoder path connected by skip connections and a bottleneck layer (Fig. 2). Instead of using convolutional elements in our network, we draw inspiration from Swin UNETR [Hatamizadeh et al., 2021], which uses Transformer blocks [Vaswani et al., 2017] in the encoder path but convolutional layers in the decoder path. We opt for a symmetric architecture where both encoder and decoder use *global-to-local* (G2L) windowed-attention blocks [Van der Goten and Smith, 2022] to avoid dependence on an extensive layering for achieving substantial spatial context size. This approach not only effectively addresses the non-local nature of motion artifacts but also reduces memory requirements [Van der Goten and Smith, 2022], as fewer blocks are necessary. G2L blocks are resolution-preserving, so to downsample from a resolution S^3 to $(S/2)^3$, we subdivide the representation into non-overlapping groups of voxels of size 2^3 , and project the eight voxels to a single number via a (shared) fully-connected layer.

Self-Supervised Training

We first pre-train MAMOC in a self-supervised manner using *masked autoencoding* in a similar manner to approaches like MAE [He et al., 2022] and Paella [Rampas et al., 2022]. We randomly mask portions of the input data by subdividing an input scan $x \in \mathbb{R}^{S \times S \times S}$ into non-overlapping blocks of size B . We then sample a *keep probability* p for each scan in the batch from a pre-defined range of values (i.e., the unit interval) and mask out *exactly* $\lceil (1-p) \cdot (S/B)^3 \rceil$ blocks. To guarantee an exact number of masked-out blocks, rather than only in expectation, we generate random permutations over the set of block indices, followed by thresholding. All voxels in a masked-out block are set to zero. The objective of the network is to reconstruct these hidden segments, encouraging the model to learn the underlying structure of clean MRI data. We

(a)

Method	128 ³		256 ³	
	PSNR \uparrow	SSIM \uparrow	PSNR \uparrow	SSIM \uparrow
AntsPy	24.841 \pm 1.407 (***)	0.863 \pm 0.025 (***)	27.350 \pm 1.652 (***)	0.880 \pm 0.029 (***)
MCFLIRT	32.492 \pm 1.332 (***)	0.942 \pm 0.028 (***)	35.374 \pm 2.407 (*)	0.945 \pm 0.033 (***)
V-Net	34.680 \pm 0.924 (***)	0.845 \pm 0.063 (***)	34.431 \pm 1.675 (***)	0.602 \pm 0.063 (***)
W-G2L-ART	36.082 \pm 1.946 (***)	0.979 \pm 0.010 (ns)	36.034 \pm 1.956 (ns)	0.963 \pm 0.014
MAMOC	37.118 \pm 1.683	0.980 \pm 0.011	36.041 \pm 1.977	0.959 \pm 0.020 (ns)

(b)

Method	128 ³		256 ³	
	SNR \uparrow	CNR \uparrow	SNR \uparrow	CNR \uparrow
AntsPy	6.785 \pm 0.563 (***)	1.452 \pm 0.175 (***)	6.950 \pm 0.378 (***)	1.675 \pm 0.210 (***)
MCFLIRT	7.297 \pm 0.453	1.550 \pm 0.149 (***)	7.297 \pm 0.501 (***)	1.787 \pm 0.221 (**)
V-Net	6.924 \pm 0.302 (***)	1.374 \pm 0.100 (***)	6.310 \pm 0.364 (***)	1.565 \pm 0.128 (***)
W-G2L-ART	6.946 \pm 0.471 (***)	1.473 \pm 0.147 (***)	6.974 \pm 0.405 (***)	1.585 \pm 0.165 (***)
MAMOC	7.222 \pm 0.494 (ns)	1.648 \pm 0.120	7.682 \pm 0.377	1.800 \pm 0.147

Figure 3: **(a)** We compare how well motion-corrected scans produced by each method are able to reconstruct motion-free scans on MR-ART. **(b)** Signal-to-noise ratios (SNR) and contrast-to-noise ratios (CNR) as estimated by MRIQC (Markers for statistical significance: '***' for $p < 0.01$, '**' for $p < 0.05$, '*' for $p < 0.1$, 'ns' for $p \geq 0.1$)

calculate the reconstruction loss using \mathcal{L}_2 . This self-supervision technique facilitates the learning of rich data representations by challenging the model to predict missing information [He et al., 2022]. We apply this process on three high-quality datasets that lack motion artifacts: ADNI [Wyman et al., 2013], OASIS-3 [LaMontagne et al., 2019], and IXI [Brain Development.org, 2023].

Transfer Learning

While self-supervision enables the network to learn rich features of high-quality MRI scans, it does not provide the model with understanding of motion artifacts or how to remove them. Thus, we fine-tune the model using real motion artifacts from MR-ART. We sample moderately and heavily motion-affected scans and train the model to reconstruct the clean (motion-free) scan of the same subject. We continue to employ masking in this phase for two reasons: (1) it acts as a regularization, improving performance and stabilizing training; (2) masked reconstruction allows the model to learn to handle small misalignments in registration between the clean scan and motion-affected scans to improve the restoration quality.

Test-Time Prediction

We propose a type of test-time augmentation to improve reconstruction in MAMOC. At inference, rather than fixing the keep probability to 1.0, we choose a specific p (constrained to the interval defined before) and perform L passes per scan. We then average the predictions. For practical purposes, this is equivalent to repeating a single scan L times over the batch dimension, so in effect the throughput for a single scan is unchanged if sufficient memory is available. By default, we set $p = 0.6$. Empirical tests to determine this hyperparameter are provided in the *Appendix*.

4 Experiments

Baseline Methods

We benchmark MAMOC against both traditional and deep learning-based artifact correction methods. MCFLIRT [Jenkinson et al., 2002] is a widely-used MC tool that accepts both fMRI and structural MRI scans. ANTsPy [Tustison et al., 2021] is a recently proposed MRI framework that offers MC capabilities. W-G2L-ART [Van der Goten and Smith, 2022] is a Transformer-based artifact correction architecture that uses a wide range of synthetic artifact classes to enable supervised learning. Furthermore, in order to rule out that the MC task can effectively be addressed by merely training in a supervised manner on MR-ART, we compare MAMOC against a V-Net [Milletari et al., 2016]. The V-Net is trained by using motion-affected MR-ART scans as inputs and is tasked to minimize the \mathcal{L}_2 error w.r.t. to the clean, same-subject MR-ART scan. W-G2L-ART is trained using synthetic artifacts on ADNI, OASIS-3, and IXI. MCFLIRT and ANTsPy use rigid and non-rigid body transformations and as such do not require training data.

Data & Preprocessing

We standardized the resolution of all datasets to 256^3 , equivalent to a voxel size of 1mm^3 , to ensure consistency across the board. Because MR-ART has been de-identified using a defacing technique (PyDeface [Gulban et al., 2022]), we apply the very same method to ADNI, OASIS-3 and IXI for the sake of consistency. The ADNI [Wyman et al., 2013] data used in the preparation of this article were obtained from the Alzheimer’s Disease Neuroimaging Initiative database (adni.loni.usc.edu). ADNI was launched in 2003 as a public-private partnership, led by Principal Investigator Michael W. Weiner, MD. The primary goal of ADNI has been to test whether serial magnetic resonance imaging (MRI), positron emission tomography (PET), other biological markers, and clinical and neuropsychological assessment can be combined to measure the progression of mild cognitive impairment (MCI) and early Alzheimer’s disease (AD). For up-to-date information, see www.adni-info.org. A complication with the MR-ART dataset is the lack of spatial alignment among scans of the same subject, complicating the application of traditional voxel-to-voxel loss metrics. To mitigate this issue, we adopted a tailored registration approach: a two-stage process for ADNI, OASIS-3 and IXI, and a more complex three-stage process for MR-ART. This involved initially co-registering any three scans from the same subject within MR-ART, followed by intra-dataset registration across different subjects. The final phase involved co-registering scans across all datasets to achieve uniformity. We use the SyN algorithm [Avants et al., 2008], a non-linear diffeomorphic registration method in all steps. In order to do away with the need of having to rely on a single fixed template, we use the template-building algorithm from ANTs [Avants et al., 2010] on the to-be-registered scans prior to co-registration. All scans are subsequently intensity normalized across all datasets using least squares normalization [Reinhold et al., 2019]. In a final step, we again resample the scans to resolution 128^3 (voxel size 2mm^3) to allow additional comparisons. We randomly partitioned MR-ART into a 70-30 train-test split by subjects.

To enable a fair comparison, we scale the model complexity of each model to fully occupy the 24 GiB GPU memory of an NVIDIA RTX 4090 with a batch size of 4. To reduce memory requirements, we apply the following techniques: Training with automatic mixed precision [Micikevicius et al., 2018], graph compilation via the *Inductor* backend [Ansel et al., 2024], and using the memory-friendly Lion [Chen et al., 2023] optimizer.

Reconstruction Quality Analysis

To measure reconstruction quality we compare the motion-corrected output from the various models to the motion-free scan from the MR-ART test set. We report the *peak signal-to-noise ratio* (PSNR) as well as the *structural similarity index* (SSIM), two metrics commonly used

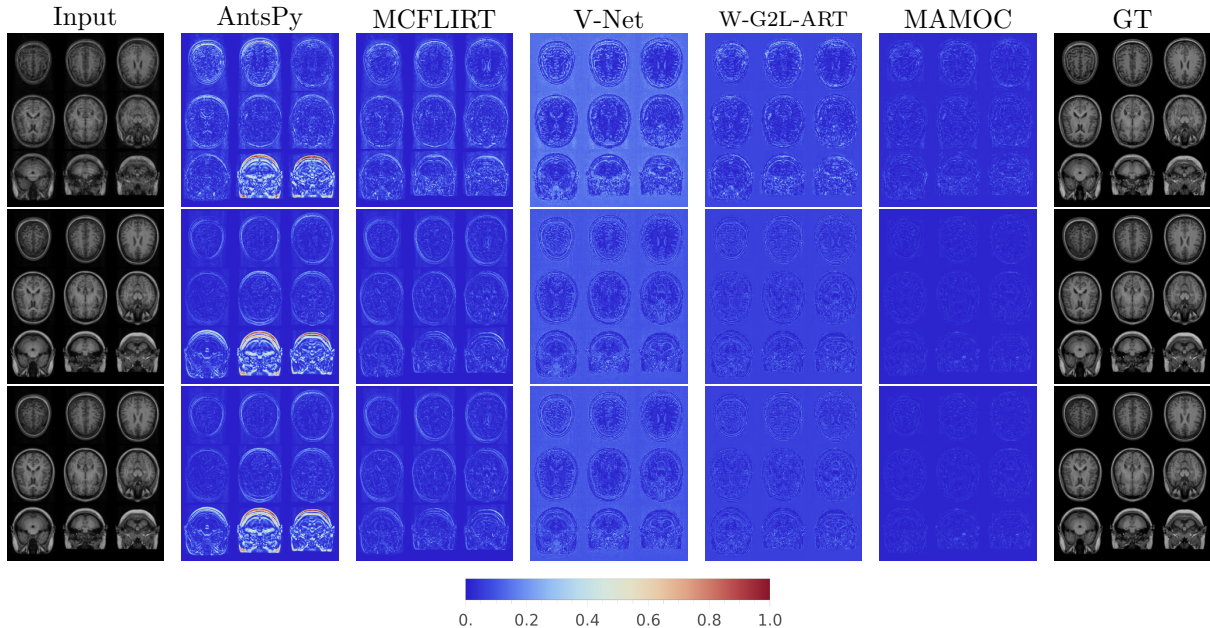


Figure 4: **Difference Maps.** We visualize the reconstruction quality with absolute difference between the outputs of various models and the ground-truth (GT), i.e., motion-free scans, given the same motion-affected inputs. Each row of difference maps is normalized as a group w.r.t. the unit interval, with lower values indicating better reconstruction quality and greater similarity to the ground truth.

to quantify visual reconstruction quality. The results reported in Fig. 3 (a) showcases that MAMOC outperforms the other methods, in most cases by a significant margin. The lone exception is W-G2L-ART on 256^3 resolution volumes, as measured by PSNR, which outperforms MAMOC by a very small margin. Visual depictions of the reconstruction quality as well as difference maps between the output of the various correction methods and the motion-free scan are provided in Fig. 4.

Image Quality Analysis

We use the *MRI Quality Control* (MRIQC) framework [Esteban et al., 2017] to gauge the image quality of motion-affected, motion-free and motion-corrected scans. The framework automatically generates a wide array of image-quality metrics specifically for MRI scans. We report the *signal-to-noise* ratio (SNR) and the *contrast-to-noise* (CNR) ratio as estimated by MRIQC in Fig. 3 (b). The latter ratio measures the separation of intensity distributions corresponding to gray and white matter. We observe that MAMOC attains the highest SNR value with respect to the 256^3 resolution and is only second to MCFLIRT in terms of the 128^3 resolution.

Subcortical Brain Segmentation

To further validate the efficacy of MAMOC, we investigate its impact on the downstream task of brain segmentation. We utilize FASTSURFER [Henschel et al., 2020], a state-of-the-art deep learning approach for subcortical brain segmentation, and apply it to three distinct MRI scans of the same subject: a motion-free scan (x_{MF}), a motion-affected scan (x_{MA}), and a motion-corrected scan (x_{MC}). The metric $\text{Dice}(x_{MF}, x_{MC}) - \text{Dice}(x_{MF}, x_{MA})$ is employed to quantify the enhancement in segmentation performance when using the motion-corrected scan compared to the motion-affected scan. The results are presented in Figure 5. While some motion correction methods fail to consistently improve downstream segmentation performance, MAMOC is

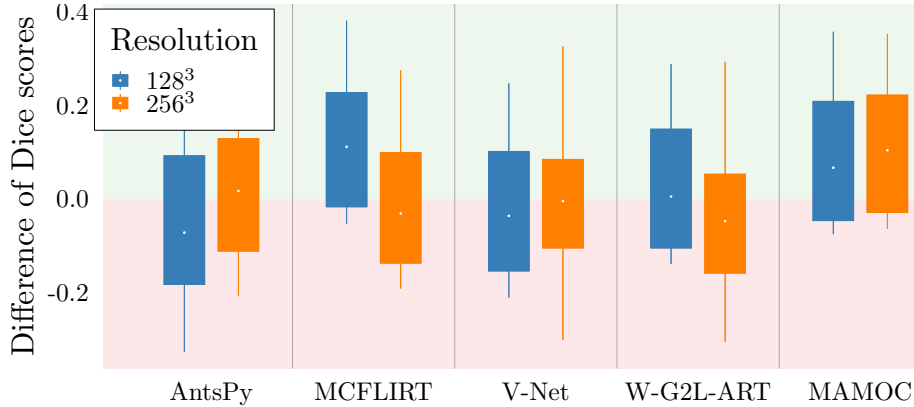


Figure 5: **Subcortical Brain Segmentation.** Positive values indicate that segmentation with FASTSURFER benefits from applying an MC algorithm on motion-affected scans. The y -axis denotes to which extent the class-averaged (96 classes) Dice score improves if an motion-affected scan is motion corrected. See text for details.

notably the only method that consistently improves improves brain segmentation outcomes in the presence of motion artifacts. This is important since subcortical brain segmentation deals with the identification of small structures that can easily be missed if a scan is affected by artifacts.

5 Conclusion

Our study introduced MAMOC, a self-supervised approach employing masked autoencoding for MRI motion artifact correction. This work stands out as the first to assess motion correction techniques against real-world motion artifacts on the MR-ART dataset. The results demonstrate MAMOC’s efficacy in generating high-resolution, motion-corrected MRI images and its superior performance over existing methods across various metrics, including PSNR and SSIM, and furthermore in enhancing subcortical brain segmentation. A key aspect of MAMOC is its use of masked autoencoding not only during training but also at inference time, which contributes to improved reconstruction quality. This approach, combined with the ability to process images at native resolution, ensures high-quality correction of motion artifacts. MAMOC can, in principle, also be trained for use in other volumetric medical imaging modalities such as CT/EEG or PET. Its efficiency on consumer-grade hardware and applicability to various imaging modalities underscore its potential for broader clinical and research applications.

Acknowledgements

Data collection and sharing for this project was funded by the Alzheimer’s Disease Neuroimaging Initiative (ADNI) (National Institutes of Health Grant U01 AG024904) and DOD ADNI (Department of Defense award number W81XWH-12-2-0012). ADNI is funded by the National Institute on Aging, the National Institute of Biomedical Imaging and Bioengineering, and through generous contributions from the following: AbbVie, Alzheimer’s Association; Alzheimer’s Drug Discovery Foundation; Araclon Biotech; BioClinica, Inc.; Biogen; Bristol-Myers Squibb Company; CereSpir, Inc.; Cogstate; Eisai Inc.; Elan Pharmaceuticals, Inc.; Eli Lilly and Company; EuroImmun; F. Hoffmann-La Roche Ltd and its affiliated company Genentech, Inc.; Fujirebio; GE Healthcare; IXICO Ltd.; Janssen Alzheimer Immunotherapy Research & Development, LLC.; Johnson & Johnson Pharmaceutical Research & Development LLC.; Lumosity; Lundbeck; Merck & Co., Inc.; Meso Scale Diagnostics, LLC.; NeuroRx Research; Neurotrack Technologies; Novartis Pharmaceuticals Corporation; Pfizer Inc.; Piramal Imaging; Servier; Takeda Pharmaceutical Company; and Transition Therapeutics. The Canadian Institutes of Health Research is providing funds to support ADNI clinical sites in Canada. Private sector contributions are

facilitated by the Foundation for the National Institutes of Health (www.fnih.org). The grantee organization is the Northern California Institute for Research and Education, and the study is coordinated by the Alzheimer's Therapeutic Research Institute at the University of Southern California. ADNI data are disseminated by the Laboratory for Neuro Imaging at the University of Southern California.

References

- J. Ansel, E. Yang, H. He, N. Gimelshein, A. Jain, M. Voznesensky, B. Bao, P. Bell, D. Berard, E. Burovski, G. Chauhan, A. Chourdia, W. Constable, A. Desmaison, Z. DeVito, E. Ellison, W. Feng, J. Gong, M. Gschwind, B. Hirsh, S. Huang, K. Kalambarkar, L. Kirsch, M. Lazos, M. Lezcano, Y. Liang, J. Liang, Y. Lu, C. K. Luk, B. Maher, Y. Pan, C. Puhersch, M. Reso, M. Saroufim, M. Y. Siraichi, H. Suk, S. Zhang, M. Suo, P. Tillet, X. Zhao, E. Wang, K. Zhou, R. Zou, X. Wang, A. Mathews, W. Wen, G. Chanan, P. Wu, and S. Chintala. PyTorch 2: Faster Machine Learning Through Dynamic Python Bytecode Transformation and Graph Compilation. In *Proceedings of the 29th ACM International Conference on Architectural Support for Programming Languages and Operating Systems, Volume 2*, volume 2 of *ASPLOS '24*, pages 929–947, New York, NY, USA, apr 2024. Association for Computing Machinery. ISBN 9798400703850. doi: 10.1145/3620665.3640366. URL <https://dl.acm.org/doi/10.1145/3620665.3640366>.
- B. B. Avants, C. L. Epstein, M. Grossman, and J. C. Gee. Symmetric diffeomorphic image registration with cross-correlation: evaluating automated labeling of elderly and neurodegenerative brain. *Medical image analysis*, 12(1):26–41, 2008.
- B. B. Avants, P. Yushkevich, J. Pluta, D. Minkoff, M. Korczykowski, J. Detre, and J. C. Gee. The optimal template effect in hippocampus studies of diseased populations. *Neuroimage*, 49(3):2457–2466, 2010.
- Brain Development.org. Ixi dataset, 2023. URL <https://brain-development.org/ixi-dataset/>.
- X. Chen, C. Liang, D. Huang, E. Real, K. Wang, Y. Liu, H. Pham, X. Dong, T. Luong, C.-J. Hsieh, Y. Lu, and Q. V. Le. Symbolic discovery of optimization algorithms, 2023.
- O. Esteban, D. Birman, M. Schaer, O. O. Koyejo, R. A. Poldrack, and K. J. Gorgolewski. Mriqc: Advancing the automatic prediction of image quality in mri from unseen sites. *PLoS one*, 12(9):e0184661, 2017.
- O. F. Gulban, D. Nielson, john lee, R. Poldrack, C. Gorgolewski, Vanessasaurus, and C. Markiewicz. poldracklab/pydeface: Pydeface v2.0.2. *software*, July 2022.
- A. Hatamizadeh, V. Nath, Y. Tang, D. Yang, H. R. Roth, and D. Xu. Swin unetr: Swin transformers for semantic segmentation of brain tumors in mri images. In *International MICCAI Brainlesion Workshop*, pages 272–284. Springer, 2021.
- K. He, X. Chen, S. Xie, Y. Li, P. Dollár, and R. Girshick. Masked autoencoders are scalable vision learners. In *Proceedings of the IEEE/CVF conference on computer vision and pattern recognition*, pages 16000–16009, 2022.
- L. Henschel, S. Conjeti, S. Estrada, K. Diers, B. Fischl, and M. Reuter. Fastsurfer—a fast and accurate deep learning based neuroimaging pipeline. *NeuroImage*, 219:117012, 2020.
- M. Herbst, J. Maclaren, J. G. Korvink, and M. Zaitsev. A practical tracking system to avoid motion artifacts. In *Proceedings 19th Scientific Meeting, International Society for Magnetic Resonance in Medicine. Montreal*, page 2683, 2011.

- M. Jenkinson, P. Bannister, M. Brady, and S. Smith. Improved optimization for the robust and accurate linear registration and motion correction of brain images. *Neuroimage*, 17(2): 825–841, 2002.
- T. Küstner, K. Armanious, J. Yang, B. Yang, F. Schick, and S. Gatidis. Retrospective correction of motion-affected mr images using deep learning frameworks. *Magnetic resonance in medicine*, 82(4):1527–1540, 2019.
- P. J. LaMontagne, T. L. Benzinger, J. C. Morris, S. Keefe, R. Hornbeck, C. Xiong, E. Grant, J. Hassenstab, K. Moulder, A. G. Vlassenko, et al. Oasis-3: longitudinal neuroimaging, clinical, and cognitive dataset for normal aging and alzheimer disease. *MedRxiv*, pages 2019–12, 2019.
- J. Lehtinen, J. Munkberg, J. Hasselgren, S. Laine, T. Karras, M. Aittala, and T. Aila. Noise2noise: Learning image restoration without clean data. *arXiv preprint arXiv:1803.04189*, 2018.
- J. Liang, J. Cao, G. Sun, K. Zhang, L. Van Gool, and R. Timofte. Swinir: Image restoration using swin transformer. In *Proceedings of the IEEE/CVF international conference on computer vision*, pages 1833–1844, 2021.
- Q. Lyu, H. Shan, Y. Xie, A. C. Kwan, Y. Otaki, K. Kuronuma, D. Li, and G. Wang. Cine cardiac mri motion artifact reduction using a recurrent neural network. *IEEE Transactions on Medical Imaging*, 40(8):2170–2181, 2021.
- J. Maclaren, M. Herbst, O. Speck, and M. Zaitsev. Prospective motion correction in brain imaging: a review. *Magnetic resonance in medicine*, 69(3):621–636, 2013.
- P. Micikevicius, S. Narang, J. Alben, G. Diamos, E. Elsen, D. Garcia, B. Ginsburg, M. Houston, O. Kuchaiev, G. Venkatesh, and H. Wu. Mixed Precision Training, feb 2018. URL <http://arxiv.org/abs/1710.03740>. arXiv:1710.03740 [cs, stat].
- F. Milletari, N. Navab, and S.-A. Ahmadi. V-Net: Fully Convolutional Neural Networks for Volumetric Medical Image Segmentation, jun 2016. URL <http://arxiv.org/abs/1606.04797>. arXiv:1606.04797 [cs].
- Á. Nárai, P. Hermann, T. Auer, P. Kemenczky, J. Szalma, I. Homolya, E. Somogyi, P. Vakli, B. Weiss, and Z. Vidnyánszky. Movement-related artefacts (mr-art) dataset of matched motion-corrupted and clean structural mri brain scans. *Scientific Data*, 9(1):630, 2022.
- C. R. Noordman, D. Yakar, J. Bosma, F. F. J. Simonis, and H. Huisman. Complexities of deep learning-based undersampled mr image reconstruction. *European radiology experimental*, 7(1):58, 2023.
- D. Rampas, P. Pernias, and M. Aubreville. A Novel Sampling Scheme for Text- and Image-Conditional Image Synthesis in Quantized Latent Spaces. *arXiv e-prints*, art. arXiv:2211.07292, Nov. 2022. doi: 10.48550/arXiv.2211.07292.
- J. C. Reinhold, B. E. Dewey, A. Carass, and J. L. Prince. Evaluating the impact of intensity normalization on MR image synthesis. In *Medical Imaging 2019: Image Processing*, volume 10949, page 109493H. International Society for Optics and Photonics, 2019.
- O. Ronneberger, P. Fischer, and T. Brox. U-net: Convolutional networks for biomedical image segmentation. In *Medical Image Computing and Computer-Assisted Intervention—MICCAI 2015: 18th International Conference, Munich, Germany, October 5-9, 2015, Proceedings, Part III 18*, pages 234–241. Springer, 2015.

- V. Spieker, H. Eichhorn, K. Hammernik, D. Rueckert, C. Preibisch, D. C. Karampinos, and J. A. Schnabel. Deep learning for retrospective motion correction in mri: A comprehensive review. *arXiv preprint arXiv:2305.06739*, 2023.
- N. J. Tustison, P. A. Cook, A. J. Holbrook, H. J. Johnson, J. Muschelli, G. A. Devenyi, J. T. Duda, S. R. Das, N. C. Cullen, D. L. Gillen, et al. The antsx ecosystem for quantitative biological and medical imaging. *Scientific reports*, 11(1):9068, 2021.
- L. A. Van der Goten and K. Smith. Wide Range MRI Artifact Removal with Transformers, Oct. 2022. URL <http://arxiv.org/abs/2210.07976>. arXiv:2210.07976 [cs, eess].
- A. Vaswani, N. Shazeer, N. Parmar, J. Uszkoreit, L. Jones, A. N. Gomez, L. Kaiser, and I. Polosukhin. Attention is all you need. In *Proceedings of the 31st International Conference on Neural Information Processing Systems*, NIPS’17, pages 6000–6010, Red Hook, NY, USA, dec 2017. Curran Associates Inc. ISBN 978-1-5108-6096-4.
- Y. Wu, X. Wang, and A. K. Katsaggelos. Motion artifact reduction in abdominal mris using generative adversarial networks with perceptual similarity loss. In *17th International Symposium on Medical Information Processing and Analysis*, volume 12088, pages 142–150. SPIE, 2021.
- B. T. Wyman, D. J. Harvey, K. Crawford, M. A. Bernstein, O. Carmichael, P. E. Cole, P. K. Crane, C. DeCarli, N. C. Fox, J. L. Gunter, et al. Standardization of analysis sets for reporting results from adni mri data. *Alzheimer’s & Dementia*, 9(3):332–337, 2013.
- J. Xiao, X. Fu, M. Zhou, H. Liu, and Z.-J. Zha. Random shuffle transformer for image restoration. In A. Krause, E. Brunskill, K. Cho, B. Engelhardt, S. Sabato, and J. Scarlett, editors, *Proceedings of the 40th International Conference on Machine Learning*, volume 202 of *Proceedings of Machine Learning Research*, pages 38039–38058. PMLR, 23–29 Jul 2023.
- M. Zaitsev, C. Dold, G. Sakas, J. Hennig, and O. Speck. Magnetic resonance imaging of freely moving objects: prospective real-time motion correction using an external optical motion tracking system. *Neuroimage*, 31(3):1038–1050, 2006.
- K. Zhang, W. Zuo, Y. Chen, D. Meng, and L. Zhang. Beyond a gaussian denoiser: Residual learning of deep cnn for image denoising. *Trans. Img. Proc.*, 26(7):3142–3155, jul 2017. ISSN 1057-7149. doi: 10.1109/TIP.2017.2662206.